Journal of Alloys and Compounds, 190 (1993) 209–217
JALCOM 428

R.f. plasma spray deposition of $LaMO_x$ (M ≡ Co, Mn, Ni) films and the investigations of structure, morphology and the catalytic oxidation of CO and C_3H_8

H. R. Khan
Forschungsinstitut für Edelmetalle und Metallchemie, W-7070 Schwäbisch Gmünd (Germany), and Department of Physics, University of Tennessee, Knoxville, 31996-1200 TN (USA)

H. Frey
Lot- und Schweißgeräte GmbH, W-7307 Aichwald (Germany)

(Received July 15, 1992)

Abstract

$LaMO_x$ (M ≡ Co, Mn, Ni) films were deposited on the Al_2O_3 supports by r.f. plasma spray deposition. These films, as well as the bulk oxide samples, were prepared by a normal pressing and sintering technique and were investigated for the morphology, phase formation and structure by using techniques such as optical microscopy, scanning electron microscopy, energy dispersive X-ray analysis, differential thermal analysis and X-ray diffraction. The temperature dependent (20–325 °C) catalytic activities such as the oxidation of CO and C_3H_8 by perovskite films are also investigated under a typical automotive operation. $LaCoO_x$ and $LaNiO_x$ films show 58% and 62% oxidation of CO respectively above 100 °C. About 40% oxidation of C_3H_8 by the $LaCoO_x$ and $LaNiO_x$ films occurs at 325 °C.

1. Introduction

The main components of auto exhausts with the Otto motor which are hazardous to health are CO, NO, SO_2 and the hydrocarbons. The chemical composition of the exhaust gas varies with the air-to-fuel ratio and the operating mode of the engine. The auto catalysts are mostly based on the noble metals such as platinum and palladium and their alloys. CO and other hydrocarbons are removed through these catalysts by oxidizing them with the excess air. The supply of noble metals is limited and there is a need to explore alternative and effective catalytic materials. There exist a variety of alternative catalytic materials but they suffer from various deficiencies. The main criteria defining the usefulness of these materials are parameters such as high chemical activity and high thermal and chemical stability in the exhaust environment. Many alternative materials such as noble metal oxides have deficiencies. A class of transition metal oxides based on the perovskite structure are found to be better oxidation and reduction catalysts than other materials. Perovskite structure oxides show all kinds of other interesting and useful physical properties such as high temperature superconductivity, diamagnetism, ferromagnetism, ferroelectricity, insulation and semiconductivity. The structure and stoichiometry of the perovskite oxides is based on $CaTiO_3$ (perovskite) and have a general formula ABO_3 where A is an alkaline metal or alkaline earth metal and B is a transition metal. Perovskites having a variety of physical properties can be synthesized by substituting different atoms at the A and B sites and by varying the chemical composition.

The cobaltate perovskites $LaCoO_3$ were first suggested as catalysts to be used in electrolysis by Meadowcroft [1] in 1970 and in auto exhausts by Libby [2] in 1971. Later these perovskites based on cobalt and manganese were investigated by several other workers [3–7] for the oxidation of CO and reduction of NO in auto exhausts. The presence of SO_2 in auto exhausts was found to poison or deactivate the catalytic properties of these catalysts. The catalytic properties of these perovskites have been investigated mostly on bulk samples. The partial substitution of noble metals such as platinum at the transition metal site of ABO_3 [8], *e.g.* $La_{0.8}Sr_{0.2}Co_{0.9}Pt_{0.1}$ dispersed on monolithic alumina supports shows catalytic activity and durability comparable with the commercially available platinum catalysts and has better resistance to lead and bromine poisoning. The catalytic activity for propene and isobutene oxidation have been studied on a series of $LaXO_3$ (X ≡

0925-8388/93/$6.00

Cr, Mn, Fe, Co, Ni) perovskite oxides by Kremenic *et al.* [9].

To design an effective solid state catalyst, the relation between the physical properties of the solid and the rate of chemical processes at the surface should be known. The properties of the perovskites which play an important role in the catalytic activity are parameters such as mixed valency states, stabilization of unusual valency states and the mobility of oxygen ions.

In this paper we report the r.f. plasma spray deposition system for the preparation of thick films of perovskites such as $LaMO_3$ (M ≡ Co, Mn, Ni) on alumina supports. The structural and morphological properties of these films as well as bulk oxides are investigated. The oxidation catalytic activity of these perovskites such as the conversion of CO and C_3H_8 to CO_2 and H_2O as a function of temperature is also investigated. To the best of our knowledge this is the first time that the oxidation catalytic acivity of perovskite oxide films deposited on alumina supports by the r.f. plasma spray technique and their characterization is reported.

2. Experimental details

The oxides La_2O_3, Co_3O_4, NiO and Mn_2O_3 were used to prepare the perovskite oxides of compositions $LaCoO_x$, $LaMnO_x$ and $LaNiO_x$. The well-mixed oxide powders were milled in a ball mill for about 4 h. This fine powder was injected into the r.f. plasma spray system to deposit thick films on the spherical alumina supports. Figure 1 shows a schematic diagram of the r.f. plasma spray system. The r.f. plasma spray source is mounted vertically with the nozzle opening into a vacuum chamber. The fine powder is injected from the top. The nozzle of the r.f. plasma source is directed onto a rotating-substrate holder, where the alumina supports are placed. The vacuum chamber was kept at an argon gas pressure of 6 mbar during the plasma spray deposition.

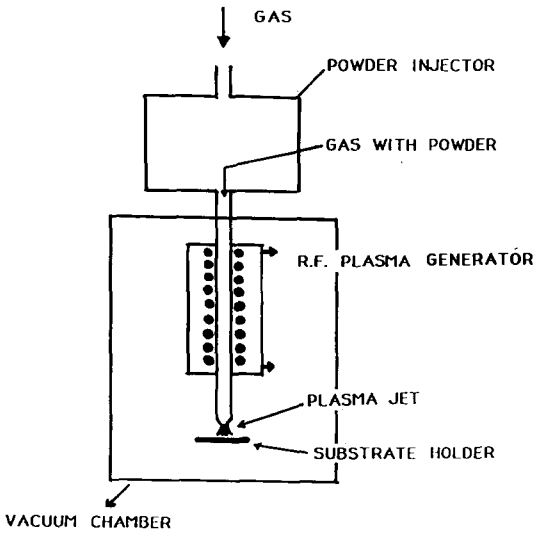

Fig. 1. R.f. plasma spray film deposition system.

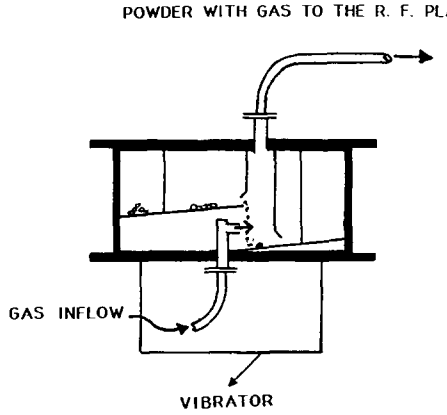

Fig. 2. Powder transport unit.

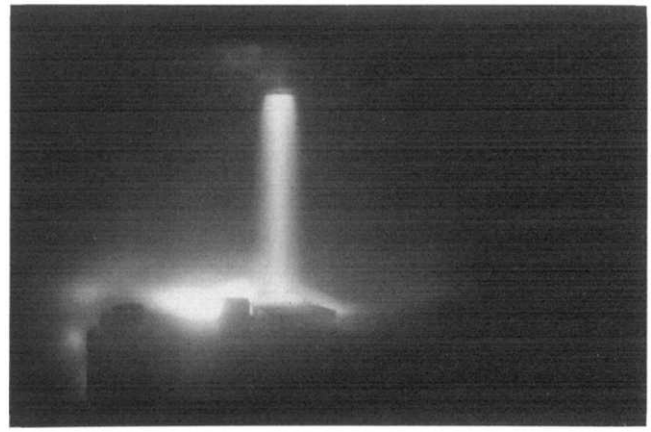

Fig. 3. Plasma jet during plasma spraying of the oxide film.

A powder transport unit (Fig. 2) is mounted on the top of the r.f. plasma generator. The powder is transported into an aerosol on a vibrating helical conveyer. The plasma gas which is argon in our case is fed into the aerosol chamber via a series of nozzles, where the fine fraction of the powder is separated from the coarse fraction and is carried with the flowing gas into the r.f. plasma generator. The rate of the argon gas flow was kept at 2 l per min. The powder feed into the aerosol chamber can be varied by the vibration amplitude of the conveyer. This powder couples to the argon gas plasma and is melted. The r.f. plasma source works on the principle of electron resonance. The plasma is generated in the quartz tube by inductive coupling of a 6 kV 2 MHz r.f. voltage. The power output of the r.f. generator is 1.5 kW and a power of about 1 kW is coupled to the plasma. The degree of ionization of the argon plasma is about 20% and the ion and electron temperatures are estimated to be 10 000 K and 50 000 K respectively. Depending upon the powder particle size, the dwell time in the plasma and the power level,

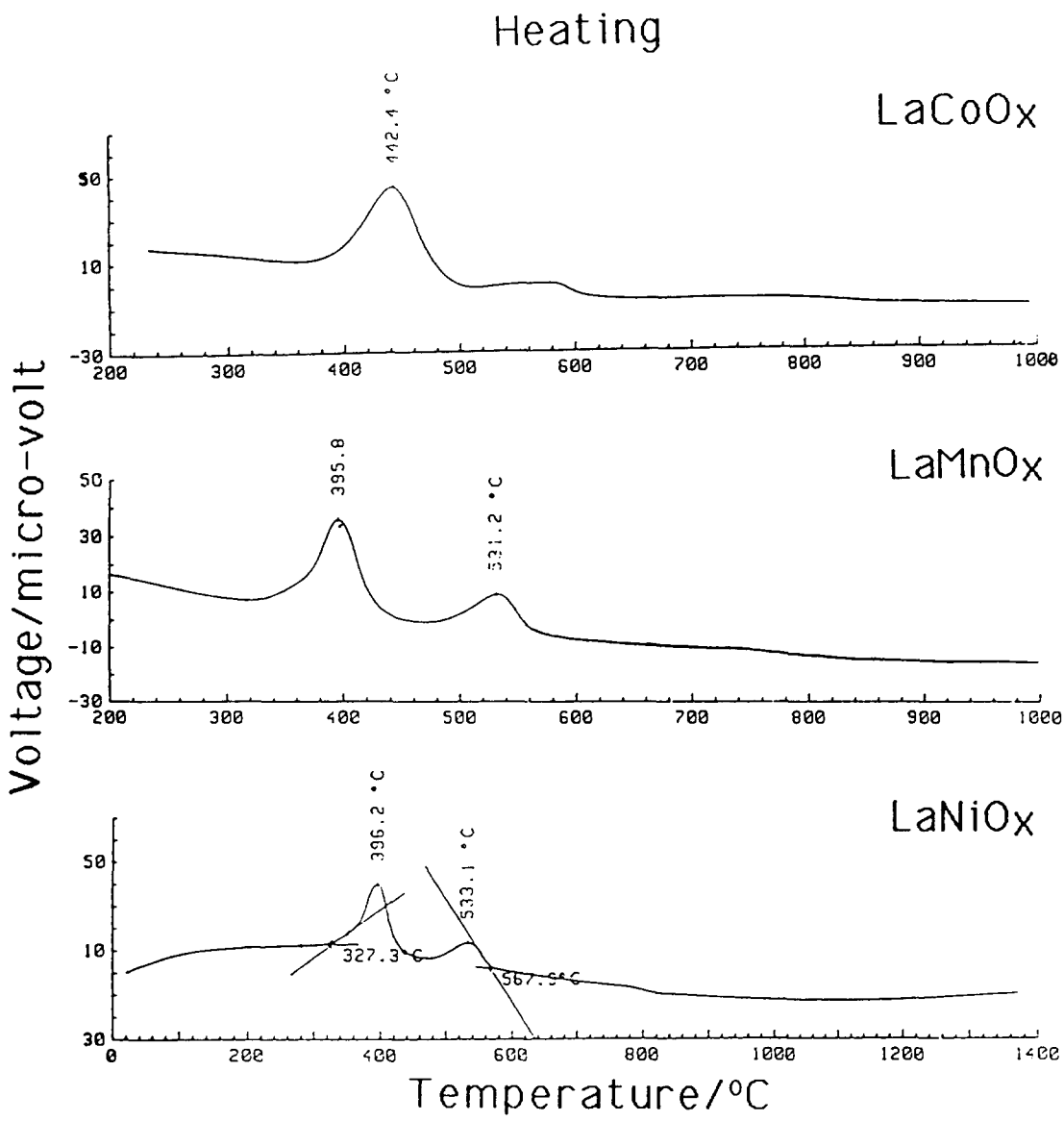

Fig. 4. Differential thermal analysis spectra for $LaCoO_x$, $LaMnO_x$ and $LaNiO_x$.

the injected powder particles are heated to temperatures in the range 1500–2000 K, which are sufficient to melt the perovskite oxide powders in the present investigation. A plasma jet during the film deposition is shown in Fig. 3. This r.f. plasma spraying has several advantages over the d.c. plasma spray technique. The most important parameter in the plasma spray technique is the time of contact between the plasma and the powder to be sprayed. For example the contact time in the case of the d.c. plasma technique depends upon how and where the powder is injected. There are two possibilities: one is that the powder is injected with the gas and the second possibility is that the powder is sprayed onto the plasma at the end. These two different methods provide different contact times and the deposited films show different physical properties. The contact time in the case of the r.f. plasma can be controlled by varying the length of the plasma. The other advantage of the r.f. plasma technique is that plasma is generated without the electrodes and the deposited films are free of impurities whereas, in the case of the d.c. plasma, impurities resulting from the electrodes cannot be avoided. Therefore the r.f. plasma technique is useful for the deposition of thick films of the materials where purity is the main criterion.

Bulk samples of perovskite oxides of the same compositions as the plasma-sprayed films were prepared by pressing the well-mixed oxide powders into pellets of 1 cm diameter under a pressure of about 12000 lbf in^{-2}. The pressed pellets were sintered in the air and oxygen atmospheres at temperatures in the range 900–1500 °C. The phase formation and the melting temperature were investigated by differential thermal analysis. The oxide-film-deposited alumina supports

TABLE 1. The X-ray analysis data and the lattice parameters of the rhombohedral phase of the bulk and film oxides heat treated in air and oxygen atmospheres

Oxide	Heat treatment			Phases[a]	Lattice parameters (rhombohedral) (Å)
	Temperature (°C)	Time (h)	Atmosphere		
$LaCoO_x$ (bulk)	1200	3	Air	R, extra	$a = 5.440 \pm 0.002$ $c = 13.078 \pm 0.007$
$LaCoO_x$ (bulk)	1200	3	O_2	R, extra	$a = 5.440 \pm 0.001$ $c = 13.084 \pm 0.006$
$LaCoO_x$ (film)	As deposited			A, $La(OH)_3$	
$LaCoO_x$ (film)	1200	3	Air	R, extra	$a = 5.439 \pm 0.005$ $c = 13.096 \pm 0.004$
$LaMnO_x$ (bulk)	1200	3	Air	R, extra	$a = 5.501 \pm 0.003$ $c = 13.431 \pm 0.015$
$LaMnO_x$ (bulk)	1200	3	O_2	R, extra	$a = 5.502 \pm 0.003$ $c = 13.450 \pm 0.017$
$LaMnO_x$ (film)	As deposited			A, $La(OH)_3$	
$LaMnO_x$ (film)	1200	3	Air	R, extra	$a = 5.479 \pm 0.003$ $c = 13.464 \pm 0.012$
$LaNiO_x$ (bulk)	1200	3	Air	R, NiO, La_2NiO_4	$a = 5.454 \pm 0.027$ $c = 13.234 \pm 0.089$
$LaNiO_x$ (bulk)	1200	3	O_2	R, NiO, La_2NiO_4	$a = 5.454 \pm 0.006$ $c = 13.234 \pm 0.094$
$LaNiO_x$ (film)	As deposited			A, $La(OH)_3$	
$LaNiO_x$ (film)	1200	3	Air	R, NiO, La_2NiO_4	$a = 5.453 \pm 0.017$ $c = 13.254 \pm 0.068$

[a]R, rhombohedral; A, amorphous; extra, small amount.

were also tempered at these temperatures to obtain the perovskite structure.

The formation of the phases, the structure, the microstructure and the chemical composition of the bulk and the oxide films were investigated by differential thermal analysis, room-temperature X-ray diffraction, optical microscopy, scanning electron microscopy (SEM) and energy-dispersive X-ray analysis (EDXA) techniques. The catalytic activities of the perovskite films on alumina supports for the simultaneous oxidation of CO and C_3H_8 were measured under conditions that were typical of automotive operation: space velocity, 20 000 h^{-1}; temperature, between 20 and 325 °C; feed composition, 0.05% C_3H_8, 0.10% CO, 4.00% O_2, 10% H_2O and balance argon gas. A flame ionization detector, OXYNOS and BINOS were used for the detection of C_3H_8, O_2 and CO respectively.

3. Results and discussion

The well-mixed oxide powders of compositions $LaCoO_x$, $LaMnO_x$ and $LaNiO_x$ were subjected to differential thermal analysis and the data is shown in the recordings of the differential thermal analysis up to 1400 °C in Fig. 4. Two endothermic reaction peaks are observed in the lower temperature range below 600 °C. No melting of these oxides occurs in these temperature ranges. Based on these data, a upper sintering temperature limit to form a perovskite phase was set to 1200 °C.

The pellets of $LaCoO_x$ composition were sintered in the temperature range 900–1200 °C in air and oxygen atmospheres and the perovskite phase formation was checked by X-ray diffraction. Tempering at 1200 °C in both air and oxygen atmospheres transforms the oxide to a perovskite structure and a small amount of extra phases was also observed. The lattice parameters of the rhombohedral perovskite phase are listed in Table 1. The X-ray diffraction pattern of the bulk oxide $LaCoO_x$ (1200 °C for 3 h in air) is shown in Fig. 5. The lattice parameters of the rhombohedral phase obtained by annealing in the oxygen atmosphere are also listed in the same table. The thickness of the plasma-spray-

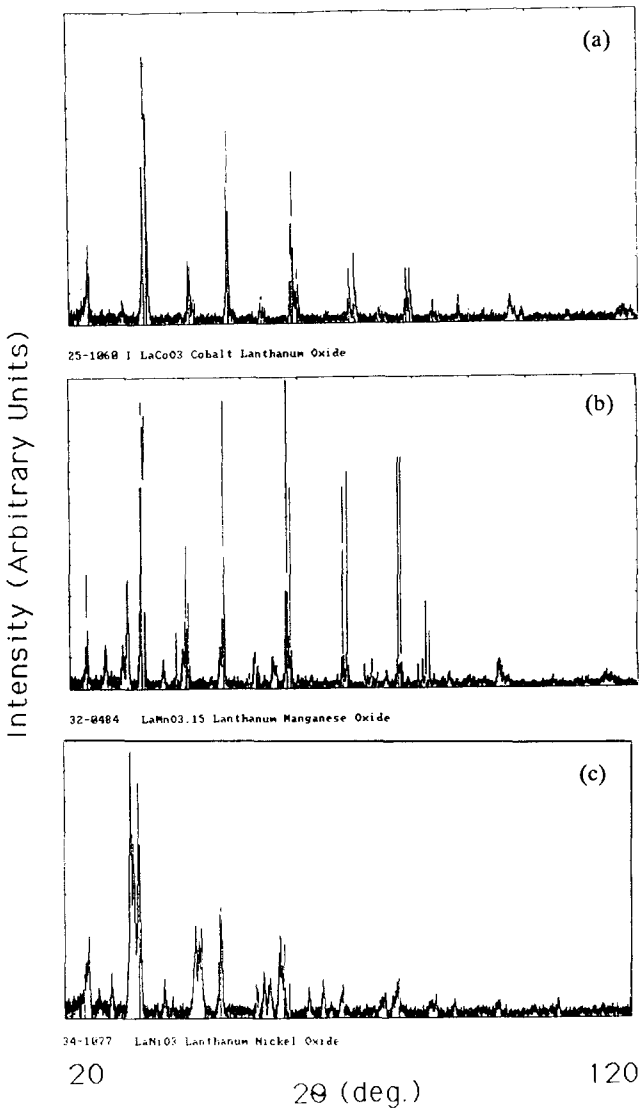

Fig. 5. X-ray diffraction patterns of the oxide pellets sintered at 1200 °C for 3 h in air: (a) $LaCoO_x$; (b) $LaMnO_x$; (c) $LaNiO_x$.

deposited film of $LaCoO_x$ on the spherical alumina supports of about 5 mm diameter varies between 1.4 and 34 μm. Optical micrographs of the cross-section of the $LaCoO_x$ film on the alumina support in the as-deposited and the heat-treated conditions are shown in Fig. 6. The X-ray diffraction of the as-deposited film shows an amorphous structure together with a crystalline structure of the $La(OH)_3$ compound (Fig. 7(a)). After heat treatment (at 1200 °C for 3 h in air), the film transforms to a rhombohedral perovskite structure (Figs. 7(b) and 7(c)) and the lattice parameters are similar to those of the sintered bulk $LaCoO_x$ which are listed in Table 1. Figure 8 shows an SEM micrograph of a $LaCoO_x$ film deposited on an alumina support. An SEM micrograph and the distribution of the lanthanum and cobalt elements in the film are shown in Fig. 9. The lanthanum and cobalt are found to be homogenously

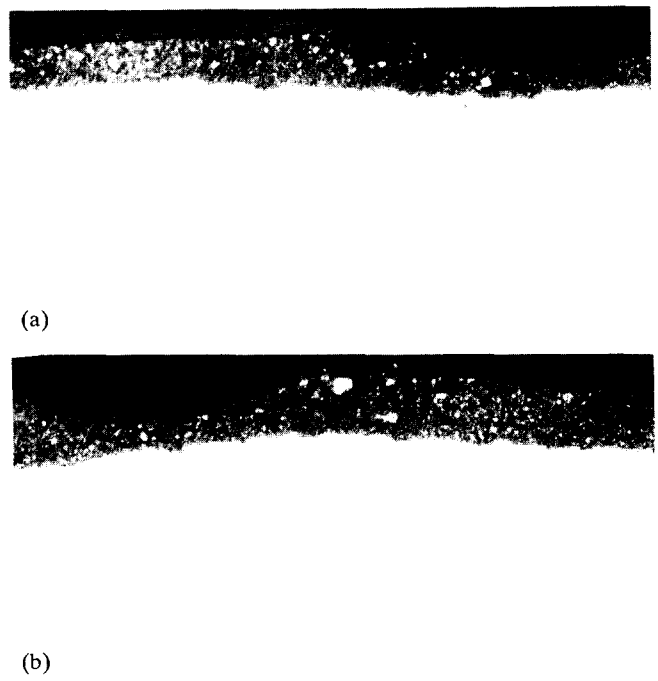

Fig. 6. Optical micrographs of the cross-section of the $LaCoO_x$ film on the alumina support: (a) as deposited; (b) heat treated.

distributed in the grains and the grain size varies between 0.5 and 1.5 μm. The film is porous and the size of the pores varies from a micron to several microns. An EDXA spectrum of the film (Fig. 10) shows that the film consists of lanthanum and cobalt elements without any other impurities.

The pellet of $LaMnO_x$ composition sintered (at 1200 °C for 3 h in air) shows a perovskite phase of composition $LaMnO_{3.15}$ as the main phase and a small amount of other phases of compositions La_2O_3 and $LaMnO_{3.00}$. An X-ray diffractogram of the $LaMnO_x$ (1200 °C for 3 h in air) is shown in Fig. 5. The annealing of this sample in the oxygen atmosphere does not change the amount or the kind of phases. The extra phases and the lattice parameters of the perovskite phase are listed in Table 1.

The thickness of the plasma-spray-deposited $LaMnO_x$ film on the alumina supports varies between 1 and 48 μm. The X-ray diffraction pattern shows the presence of amorphous and crystalline $La(OH)_3$ phases in the as-deposited condition, similiar to the $LaCoO_x$, but after annealing (at 1200 °C for 3 h in air) the film transforms to a perovskite structure. The X-ray diffraction patterns of the films in the as-deposited and the annealed conditions are shown in Fig. 11 and the extra phases together with the lattice parameters of the perovskite phase are also listed in Table 1. Figure 12 shows an SEM image and a homogenous distribution of the lanthanum and manganese elements in the grains of the $LaMnO_x$ film. The film is denser and the grains are larger than in the $LaCoO_x$ film.

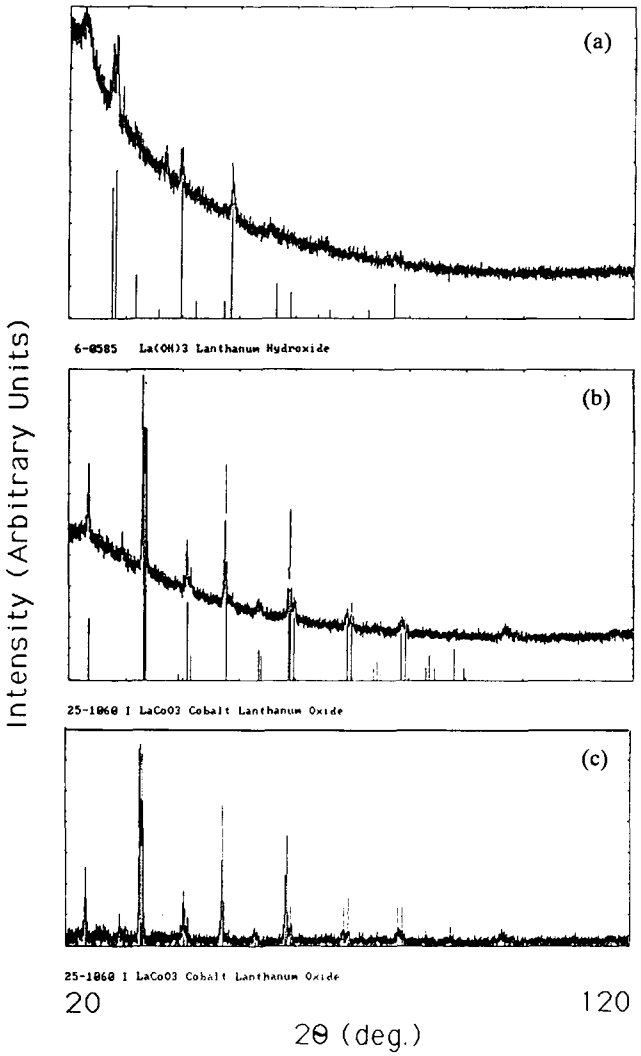

Fig. 7. X-ray diffraction patterns of $LaCoO_x$ films: (a) as deposited; (b), (c) annealed at 1200 °C for 3 h in air.

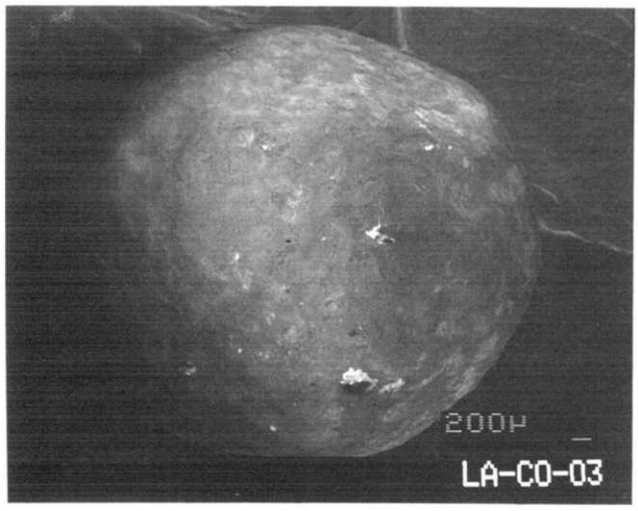

Fig. 8. SEM image of a $LaCoO_x$ film deposited on a spherical alumina support.

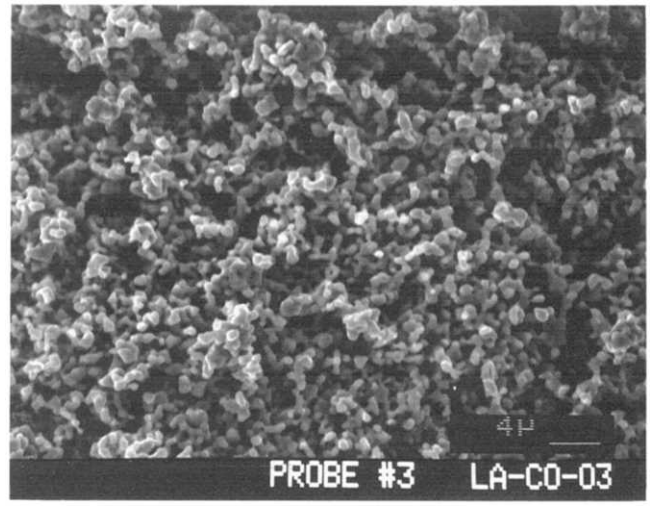

(a)

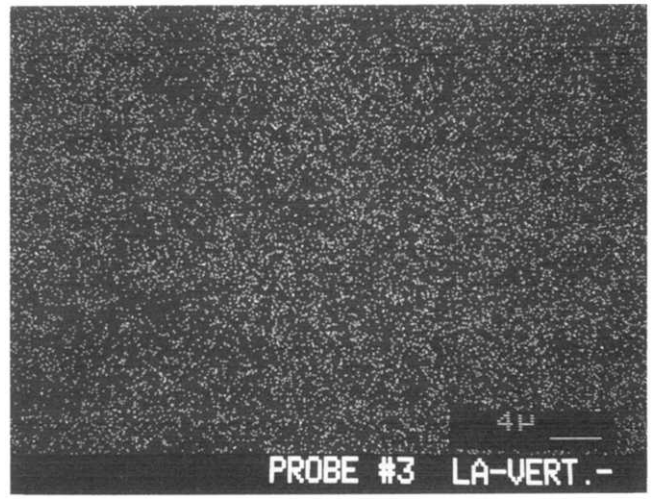

(b)

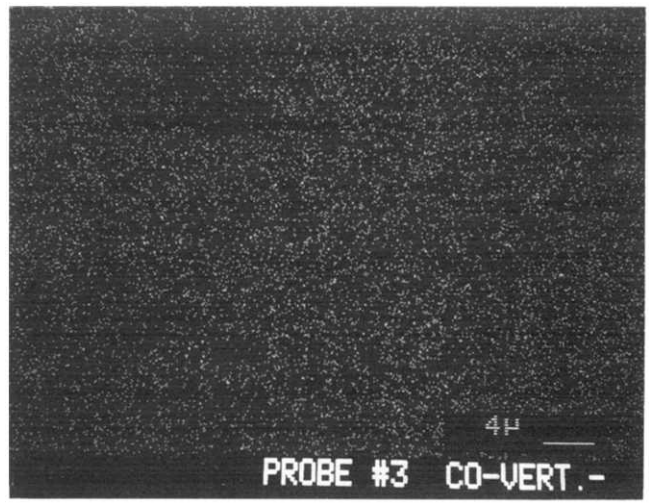

(c)

Fig. 9. (a) SEM image and (b), (c) the EDXA images of (b) lanthanum and (c) cobalt in the $LaCoO_x$ film (1200 °C for 3 h in air).

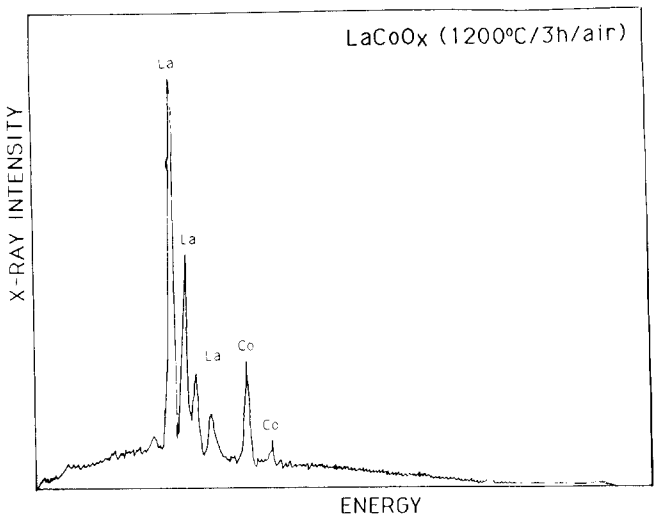

Fig. 10. EDXA spectrum of the $LaCoO_x$ film.

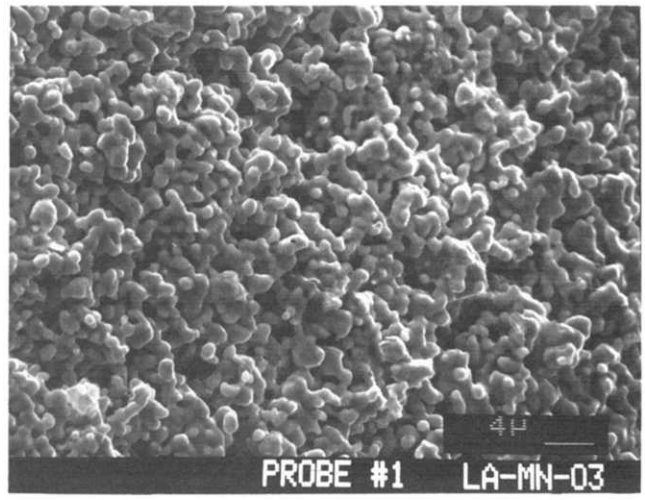

(a)

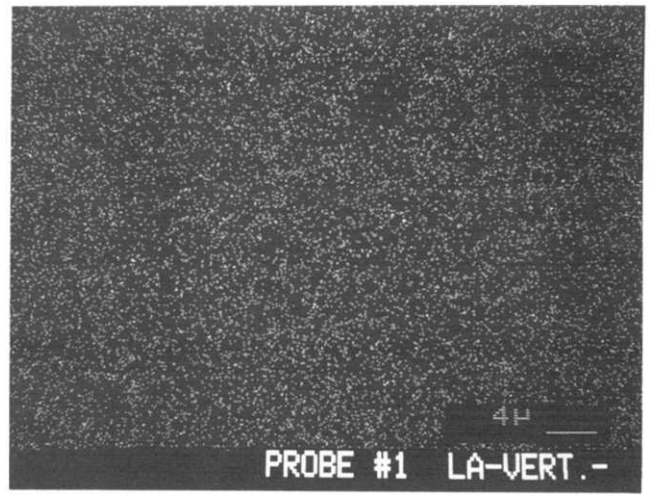

(b)

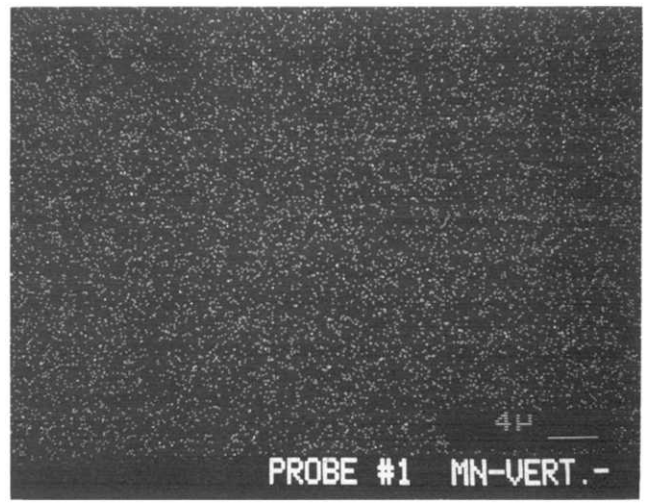

(c)

Fig. 12. (a) SEM image and (b), (c) the EDXA images of (b) lanthanum and (c) manganese in the $LaMnO_x$ film (1200 °C for 3 h in air).

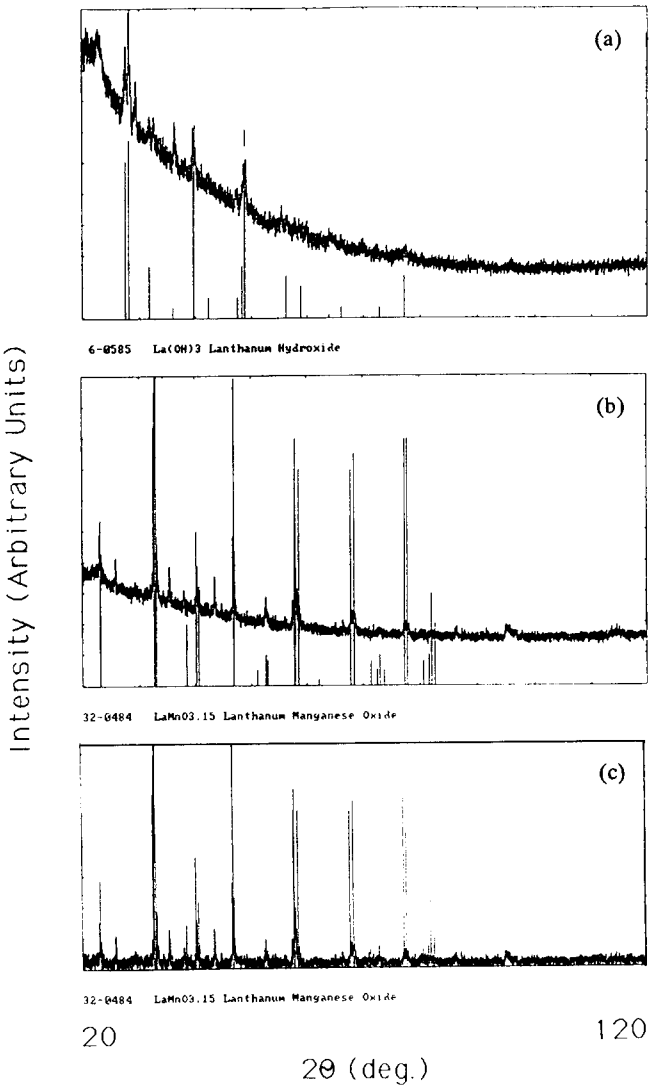

Fig. 11. X-ray diffraction patterns of $LaMnO_x$ films: (a) as deposited; (b), (c) annealed at 1200 °C for 3 h in air.

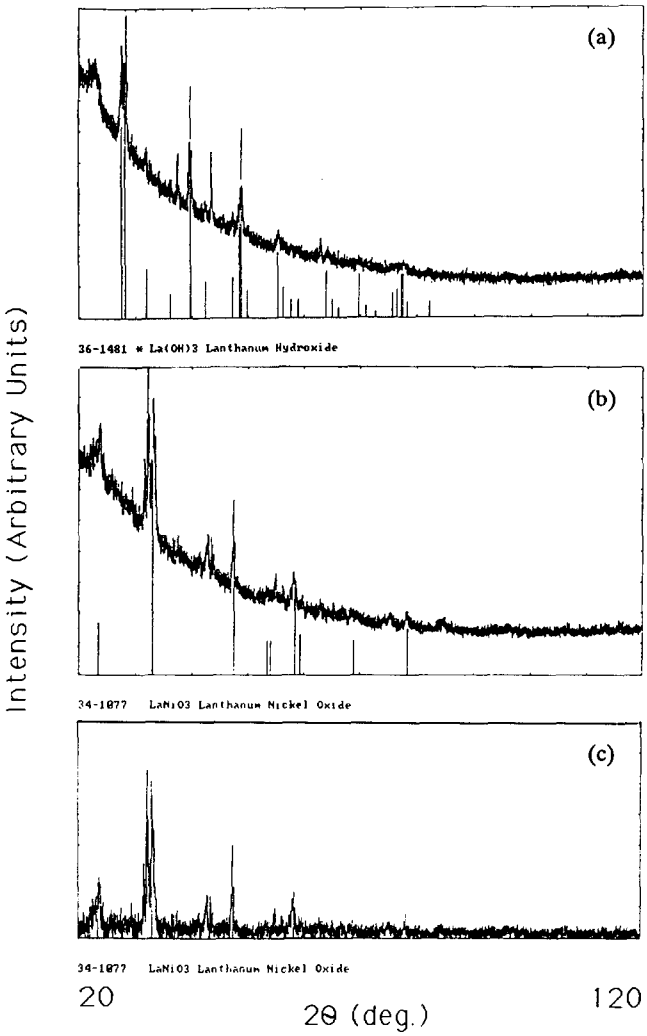

Fig.13. X-ray diffraction patterns of $LaNiO_x$ films: (a) as deposited; (b), (c) annealed at 1200 °C for 3 h in air.

The X-ray diffraction of a bulk $LaNiO_x$ (sintered at 1200 °C for 3 h in air) shows the perovskite phase as the main phase and small amounts of NiO and La_2NiO_4 as the extra phases. The X-ray diffraction pattern of the air-annealed sample is shown in Fig. 5. A heat treatment in oxygen atmosphere does not affect the amount and kinds of phase. The extra phases and the lattice parameters of the perovskite phase are also listed in Table 1. The thickness of the plasma-sprayed $LaNiO_x$ film on the alumina supports varies from 1 to 50 μm. X-ray diffraction shows the presence of amorphous and crystalline $La(OH)_3$ phases in the as-deposited condition similar to the $LaMnO_x$ but after annealing (at 1200 °C for 3 h in air), the film transforms to a perovskite structure. The X-ray diffraction patterns of the films in the as-deposited and the annealed conditions are shown in Fig. 13 and the X-ray analysis as well as lattice parameters of the perovskite phase are listed in Table 1. Figure 14 shows an SEM micrograph and

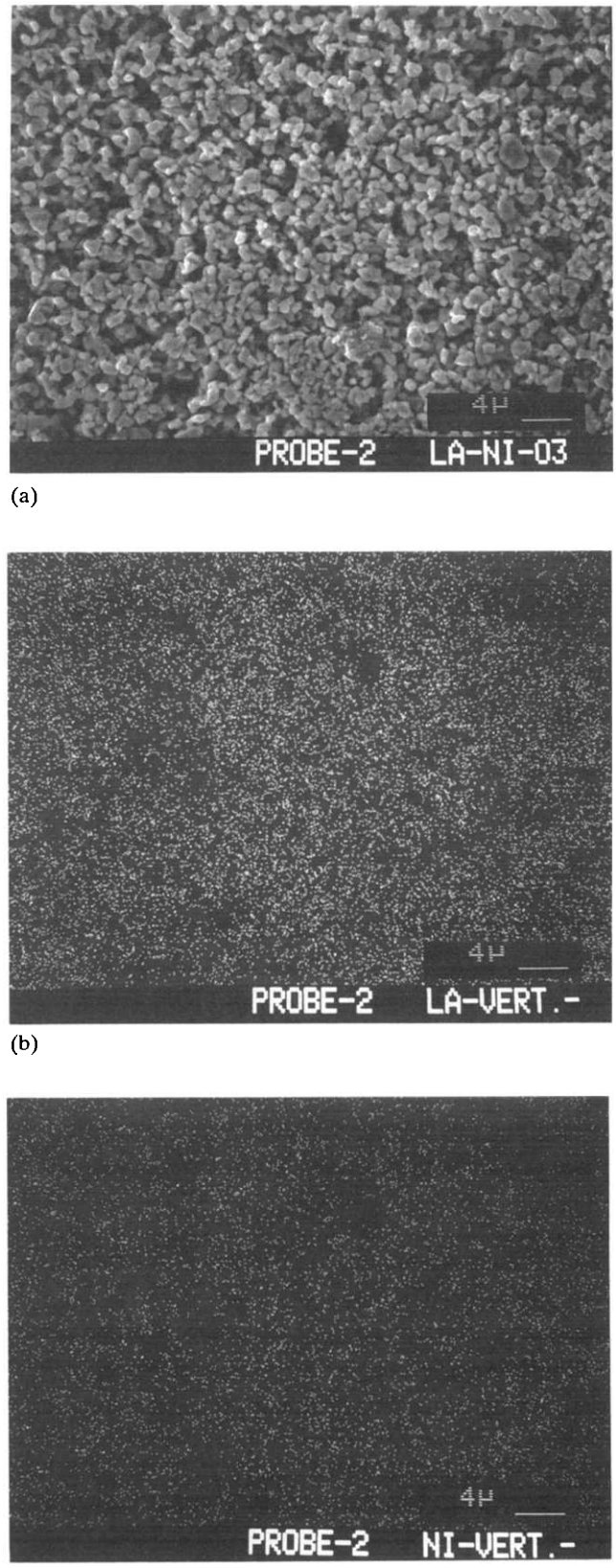

Fig. 14. (a) SEM image and (b), (c) the EDXA images of (b) lanthanum and (c) nickel using the corresponding K radiation in the $LaNiO_x$ film (1200 °C for 3 h in air).

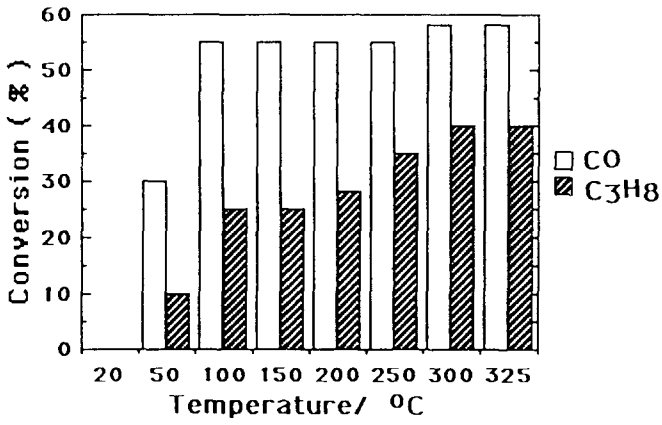

Fig. 15. Conversion percentage of CO and C_3H_8 to CO_2 and H_2O as a function of temperature by $LaCoO_x$ films on alumina supports.

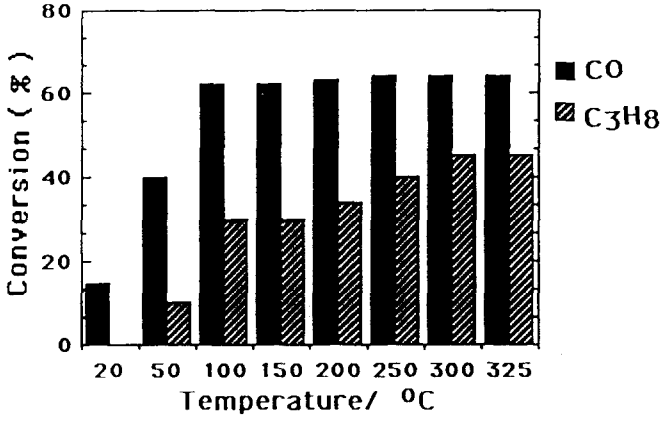

Fig. 16. Conversion percentage of CO and C_3H_8 to CO_2 and H_2O as a function of temperature by $LaNiO_x$ films on alumina supports.

the homogeneous distribution of the lanthanum and nickel elements in the grains of the $LaNiO_x$ film. The film is denser than $LaCoO_x$ but the grains are of comparable size.

The oxidation catalytic activity, *e.g.* the conversion of CO and C_3H_8 to CO_2 and H_2O by $LaCoO_x$ plasma-spray-deposited films on alumina supports (annealed at 1200 °C for 3 h in air) in the temperature range 20–325 °C, shows that conversion of CO to CO_2 at around 50 °C is 30% and, above a temperature of 100 °C, it increases slowly to 58%. Similarly the oxidation of C_3H_8 increases from 10% at 50°C to 40% at 325°C. The conversion percentage of the CO and C_3H_8 to CO_2 and H_2O as a function of temperature is shown in Fig. 15. The oxidation of CO by the plasma-sprayed $LaNiO_x$ films on the alumina supports (annealed at 1200 °C for 3 h in air) at 20 °C is about 12% and it increases to 40% at a temperature of 50 °C and 62% at 100 °C and then remains almost constant up to 325 °C. The oxidation of C_3H_8 is about 10% at a temperature of 50 °C, which increases to 30% at a temperature of 100 °C and a maximum value of about 40% is observed at a temperature of 325 °C. The conversion percentage of the CO and C_3H_8 to CO_2 and H_2O as a function of temperature is shown graphically in Fig. 16. Both the $LaCoO_x$ and the $LaNiO_x$ are perovskites of rhombohedral structure and the difference between activities of these catalysts cannot be related to their crystal structure. The surface areas of these two catalysts are comparable; therefore the difference between the catalytic activities is caused by the different solid state electronic structures of these two perovskites manifested at the surface. Temperature-dependent electrical resistivity and magnetic susceptibility measurements in order to understand the electronic structure of these oxides and its relationship to catalytic activity are under investigation.

Acknowledgments

This work was supported by Bundesministerium für Forschung und Technologie, Germany, under Grant 03C256BO. The authors are grateful to Firma W. C. Heraues, Hanau, Germany, for measurements of catalytic activities.

References

1 D.B. Meadowcroft, *Nature, 226* (1970) 847.
2 W. F. Libby, *Science, 171* (1971) 499.
3 G. W. Berkstresser, *Ph.D. Thesis*, University of Southern California.
4 Y. F. Y. Yao, *J. Catal., 36* (1975) 266.
5 R. J. H. Voorhoeve, J. P. Remeika, P. E Freeland and B. T. Matthias, *Science, 177* (1972) 353.
6 R. J. H. Voorhoeve, J. P. Remeika, and D. W. Johnson, Jr., *Science, 180* (1973) 62.
7 R. J. H. Voorhoeve, J. P. Remeika, L. E. Trimble, A. S. Cooper, F. J. Disalvo and P. K. Gallagher, *J. Solid State Chem. 14* (1975) 395.
8 A. Lauder, *US Patent 3,897,367 (1975)*; Rep. PLMR 6-75, (E.I. Dupont Petroleum Laboratory).
9 G. Kremenic, J. M. L. Nieto, J. M. D. Tascon and L. G. Tejuca, *J. Chem. Soc., Faraday Trans., 81* (1985) 939–949.